Original Research

Characterization of N-Ethyl-N-Nitrosourea-Induced Malignant and Benign Breast Tumors in Rats by Using Three MR Contrast Agents

Min-Ying Su, PhD,[1] Zhiheng Wang, PhD,[1] Philip M. Carpenter, MD,[2] Xiaoyan Lao, MD,[1] Andreas Mühler, MD,[3] and Orhan Nalcioglu, PhD[1]

A carcinogen (N-ethyl-N-nitrosourea)-induced animal tumor model was established to grow malignant and benign breast tumors. In each tumor the pharmacokinetic characteristics were measured by using three contrast agents, gadolinium-diethylene-triamine-pentaacetic acid (Gd-DTPA; <1 kD), Gadomer-17 (35 kD), and albumin-Gd-DTPA (70–90 kD). Infiltrating ductal carcinomas (IDC) with low, medium, and high Scarf-Bloom-Richardson grades and fibroadenomas (FA) were analyzed. We found that Gd-DTPA could differentiate between FA and malignant tumors, but not between malignant tumors of low and high grades. In contrast, the intermediate size agent Gadomer-17 could differentiate between high-grade and low-grade IDC, but not between low-grade IDC and FA due to their similar enhancement patterns (despite their different origins). The largest agent, albumin-Gd-DTPA, was capable of differentiating both, but the low contrast-to-noise ratio was its major technical concern. The results in this breast tumor model suggest that macromolecular agents provide useful information for differential diagnosis among IDCs of various grades, but they do not provide superior information than Gd-DTPA for differential diagnosis between IDC and FA. J. Magn. Reson. Imaging 1999;9:177–186. © **1999 Wiley-Liss, Inc.**

Index terms: malignant and benign breast tumors; MR contrast agents; pharmacokinetic analysis; dynamic contrast-enhanced MRI

DYNAMIC CONTRAST-ENHANCED magnetic resonance imaging (MRI) in breast imaging has demonstrated an excellent sensitivity but a questionable specificity in the diagnosis of primary (1–9) and recurrent (10–14) cancer since its introduction more than a decade ago. In the diagnosis of primary breast cancer, the technique suffers from a significant overlap between the enhancement patterns measured in malignant and benign (especially fibroadenoma) lesions. There is a high false-positive rate due to rapidly enhanced benign tumors (3,4,7). In the diagnosis of recurrent breast cancer after breast-conserving therapy, the technique suffers from the post-therapeutic changes that may also exhibit strong enhancement that is not distinguishable from the recurrent cancer (10,11).

To date the MR contrast agents approved for clinical studies have all had small molecular weights. As such, they are distributed into the extracellular space in the whole body (except in the central nervous system) and are thus categorized as extracellular agents. A benign or malignant tumor that has a high extracellular volume will exhibit a strong enhancement in contrast-enhanced MRI. The major problem with small molecules is the non-selectivity of vessels for their passage. If a larger molecule is used instead, it may selectively pass across a leaky vessel (e.g., capillary of discontinuous or sinusoidal type), but not a non-leaky vessel (e.g., continuous type) (15). Therefore, a blood pool agent that mainly stays intravascular but may leak out from hyperpermeable vessels may provide information on the leakage status of vessels. Vascular permeability is an important factor in a tumor that is known to correlate with a tumor's growth, its ability to metastasize, and its response to treatment (15–17). Adam et al (18) have shown that in spontaneous breast tumors in dogs, the use of a new blood pool agent [24-gadolinium-ethylene-triamine-pentaacetic acid (24-Gd-DTPA)-cascade-polymer] could reveal a significant difference between the enhancement kinetics of carcinomas and benign tumors, but not the small agent Gd-DTPA. They observed that there was a higher uptake of the blood pool agent in carcinomas than in benign tumors, presumably due to leaky vessels. We have also shown that the uptake of two blood pool agents (24-Gd-DTPA-cascade-polymer and polylysine-Gd-DTPA) was higher in a faster growing tumor than in a more slowly growing tumor, but not that of Gd-DTPA (19).

In this study we investigated the enhancement kinetics of carcinogen-induced malignant and benign breast tumors in rats, by using three contrast agents: Gd-DTPA (<1 kD), Gadomer-17 (35 kD), and albumin-Gd-DTPA (70–90 kD). The kinetics measured by using the two macromolecular contrast agents were compared

[1]Health Sciences Research Imaging Center, University of California, Irvine, California 92697.

[2]Department of Pathology, University of California, Irvine, California 92697.

[3]Diagnostic Imaging, Berlex Laboratories, Montville, New Jersey 07045.

Contract grant sponsor: State of California Breast Cancer Research Program; contract grant number: 1RB-0160.

Presented at the 6th ISMRM Meeting, 1998.

Address reprint requests to: O.N. E-mail: NALCI@UCI.EDU

Received April 8, 1998; Accepted August 4, 1998.

with those measured by the small agent Gd-DTPA. The enhancement kinetics were further analyzed using a pharmacokinetic model to derive the fitting parameters and separate the vascular and extravascular kinetics (20). The measured enhancement kinetics from the whole tumor, or the separated intra- and extravascular kinetics, were compared to investigate whether they could be used to differentiate between benign and malignant tumors, and/or to differentiate between low-grade and high-grade malignant tumors. The results obtained by using the three contrast agents were compared to investigate whether macromolecular contrast agents are more sensitive than the clinically used small contrast agents in differential diagnosis, so that a higher specificity can be achieved with the blood pool agents.

MATERIALS AND METHODS

Tumor Model

A carcinogen, N-ethyl-N-nitrosourea (ENU)-induced breast tumor model was employed in this study (21). ENU (45–180 mg/kg) was injected intraperitoneally into 30-day-old specific pathogen-free (SPF) Sprague-Dawley rats to induce tumors. Fifty animals were used in the study. ENU was synthesized in our laboratory, and its chemical structure ($C_3H_7N_3O_2$) was confirmed by mass spectrometry (22). The synthesized crystal powder was dissolved in a solution of pH 4.0 just before use. Tumors appeared gradually beginning at 4 months after injection of ENU. They were identified in the mammary fat pads and the axillae. After the tumors had reached 1.5 cm in diameter, they were subjected to MRI studies.

MRI Experimental Protocol

The experiments were performed on a GE 1.5 T Signa scanner. The enhancement kinetics in each tumor were studied by using three contrast agents, Gd-DTPA (0.1 mmol/kg), Gadomer-17 (0.05 mmol/kg), and albumin-Gd-DTPA (0.02 mmol/kg). Gadomer-17, a synthetic dendrimeric gadolinium chelate with an apparent molecular weight of 35 kD, was provided by Schering (Berlin, Germany). Albumin-Gd-DTPA (molecular weight 70–90 kD) was synthesized at our institute. Rats were anesthetized by injecting ketamine (87 mg/kg) mixed with Rompun (13 mg/kg), and then a 25 gauge butterfly needle was inserted into the tail vein for injection of contrast agents. The animal was placed in a prone position into a 10 cm birdcage coil. A set of T_2-weighted images were taken by using a fast spin-echo sequence (TR 3 seconds, TE 112 msec, echo train 8) to identify location of tumor. Depending on the tumor size, two to three slices were prescribed to cover the tumor. One slice was prescribed through the liver. The dynamic images were acquired before and after injection of contrast agents, by using a spin-echo pulse sequence with TR/TE 140/14 msec, simultaneously from four slices (23). The other imaging parameters were: FOV (field of view) 16 cm, slice thickness 5 mm, matrix size 256×128, number of excitations (NEX) 1. The temporal resolution in the time course was 18.8 seconds, which was sufficient for the compartmental analysis according to our previous studies (unpublished data). After the imaging slices had been prescribed, dynamic acquisition was started. Gd-DTPA was injected after completing four acquisitions, and the kinetics were continuously monitored for 14 minutes. After waiting 1 hour to allow for the clearance of Gd-DTPA (more than 90%), the dynamic imaging sequence was repeated again for the Gadomer-17 study. The study of albumin-Gd-DTPA was conducted on a different day using the same protocol.

Pathology

After imaging studies had been completed, the tumor was removed and placed in B5 fixative for pathological examination. Depending on the size of each tumor, tissue samples from two to six regions were examined. The tumor diagnoses were determined by examination of hematoxylin and eosin-stained histologic sections by a pathologist with experience in breast histopathology, using established criteria for the diagnosis of tumors of the rat breast (24). In the case of infiltrating ductal adenocarcinoma (IDC), the Scarf-Bloom-Richardson grade was determined (25). In humans, a widely accepted surrogate marker of breast cancer aggressiveness are the histopathologic features of tumor differentiation, proliferation, and nuclear pleomorphism, which together form the basis of the Scarf-Bloom-Richardson grading system of IDC. Higher scores correlate with greater tumor aggressiveness and decreased survival in humans. For this reason, the Scarf-Bloom-Richardson grade was assigned to each tumor to estimate its potential for aggressiveness at the time that measurements were taken. Briefly, a score of 1–3 was assigned for degree of loss of ductal morphology, variability of nuclear size and shape, and number of mitotic figures in the area of a high-power microscopic field. Well-defined criteria for the assignment of these values have been described (25). The scores were summed to give a final score of 3–9. For the purposes of this study, tumors with values from 3 to <5, 5–7, and ≥ 7 were designated low-grade (LG), mid-grade (MG), and high-grade (HG), respectively.

Data Analysis

In each tumor the enhancement kinetics of the three contrast agents were obtained. In each imaging slice of a tumor, a region of interest (ROI) was manually outlined to cover the tumor region based on the T2-weighted image. The necrotic or edematous region (with high signal intensity) was excluded in the ROI. The signal intensities measured from the two to three ROIs from different imaging slices of the tumor were averaged to calculate a mean signal intensity. The pre-contrast signal intensity was subtracted from the post-contrast signal intensity to calculate the signal enhancement at each time point, and then a complete time course over the imaging period was obtained. Only IDCs and fibroadenomas (FAs) were analyzed in this study. According to the Scarf-Bloom-Richardson grade, the IDCs were separated into low-grade, medium-grade, and high-grade

groups, using the criteria stated earlier. All FAs were pooled into one group. In each of these four groups the measured enhancement kinetics from all tumors were averaged to calculate a mean enhancement kinetics.

Since the enhancement kinetics would be compared among the three contrast agents, which had different relaxivities and were injected at different doses, an internal reference was used to normalize these two factors. The vessels in the liver are of the sinusoidal type and thus are hyperpermeable to all three agents used in this study (15). The distribution volume of each agent in the liver was assumed to be the total extracellular volume, and the maximal enhancement in the liver was dependent on the relaxivity and dose of each agent. By normalizing the signal enhancement measured in the tumor to the maximal enhancement measured in the liver, a relative concentration time course in the tumor was obtained. A detailed justification for this procedure and reasoning has been given in a previous publication (19).

The kinetics in the tumor were analyzed with a two-compartmental pharmacokinetic model to drive three fitting parameters (V_b, V_eK_{12}, and K_{21}), where V_b is the vascular volume, V_e is the extravascular distribution volume, and K_{12} and K_{21} are the in-flux and out-flux transport rates from blood to the interstitial space, respectively. The details of the pharmacokinetic model have been described previously (20). The model is also reconcilable with several models used by other research groups (26–30). Briefly, the model assumes two compartments, vascular and extravascular, connected with in-flux and out-flux transport rates (K_{12} and K_{21}). The contrast agents in the tumor are distributed in both compartments. The respective contributions from these two compartments could be separated with the model analysis. The fractional vascular volume in the tumor could be obtained by referencing to the extracellular volume in the liver (19). Statistical analyses were performed to investigate whether the kinetics from the whole tumor or the separated intra- and extravascular kinetics could be used to differentiate between benign and malignant tumors, and/or between low-grade and high-grade malignant tumors; at what time after the contrast agent injection the differences were significant. Statistical analyses were performed using paired t-tests. The data obtained by using the three contrast agents were analyzed in the same way, and the results were compared.

RESULTS

Histologic examination of tumors excised after imaging studies revealed a total of 20 IDCs, which were characterized by abnormal proliferation of glandular tissue infiltrating the surrounding tissue. Analysis of Scarf-Bloom-Richardson grade in the IDC resulted in seven low-grade, seven intermediate-grade, and six high-grade tumors. Examples of histologic sections of low-, medium-, and high-grade IDC are shown in Fig 1–c. A total of 18 FAs were found. FAs were characterized by cytologically benign glandular cells embedded in a nodular fibrous stroma (Fig. 1d). Other types of breast tumors, including ductal carcinoma in situ (n = 2), tubular adenoma (n = 6), fibroma (n = 2), papilloma (n = 1), benign intraductal proliferation (n = 1), and other malignant tumor types (n = 4) were also found (data not shown).

Figure 2 shows the signal enhancement kinetics measured in the liver by using the three contrast agents, Gd-DTPA (0.1 mmol/kg), Gadomer-17 (0.05 mmol/kg), and albumin-Gd-DTPA (0.02 mmol/kg). The different magnitude of enhancement was due to their different relaxivities and injected doses. The different decay pattern was due to the clearance in the blood

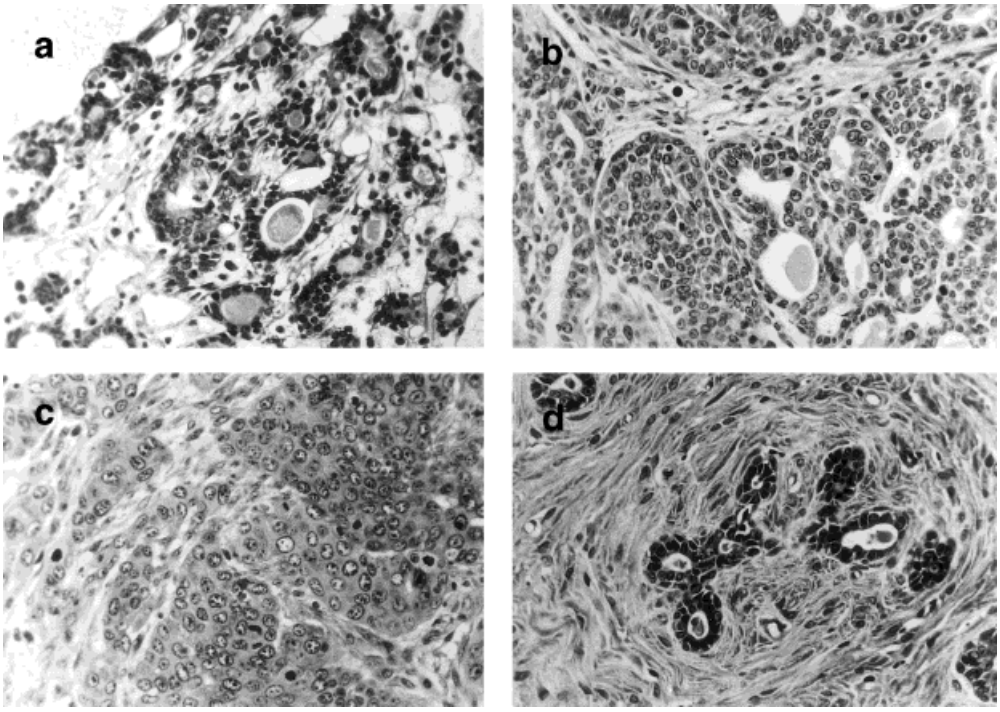

Figure 1. Photomicrographs of ENU-induced rat breast tumors (hematoxylin and eosin staining). **a:** Low-grade infiltrating ductal carcinoma, showing well-defined tubule formation, uniform nuclei, and rare mitotic figures. **b:** Medium-grade carcinoma, showing both solid and tubular areas, moderate variations in nuclear size and shape, and occasional mitoses. **c:** High-grade carcinoma, characterized by solid and infiltrating tumor without tubules, as well as marked nuclear variability with nuclear enlargement. Numerous mitotic figures are present, indicating rapid cell division. **d:** Fibroadenoma, characterized by benign, well-formed glands embedded in a fibrous stroma.

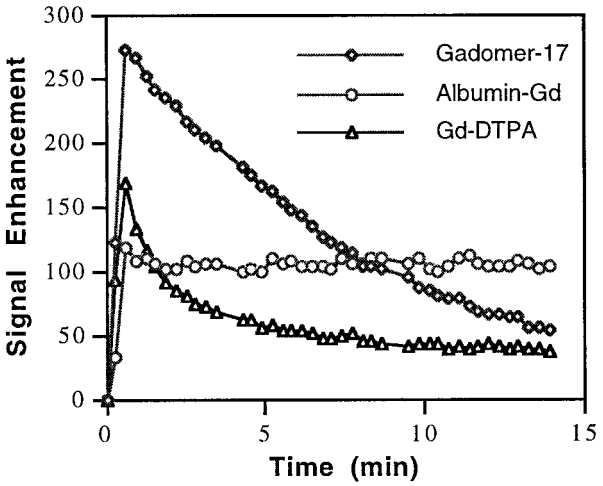

Figure 2. The signal enhancement kinetics measured in the liver by using the three contrast agents, Gd-DTPA, Gadomer-17, and albumin-Gd-DTPA. The different magnitude of enhancement was due to their different relaxivities and injected doses. The different decay pattern was determined by the distribution to the body and clearance from the kidneys; the two smaller agents could be effectively cleared from the bloodstream.

concentration, which was determined by the distribution volume in the whole body and the efficiency of the clearance via the kidneys. Enhancement of signal intensity at the second time point (0.6 minutes after injection) was used to normalize the enhancement measured in the tumor to calculate the relative concentration for comparison among the three agents. Figure 3 shows the relative concentration kinetics in the four groups, using the three different agents. The vertical axis is the relative concentration, as defined earlier. The enhancement kinetics of Gd-DTPA in FA showed a slower rise-up slope and a slower decay rate than that in IDC. The kinetics of Gd-DTPA in the three IDC groups (low-grade, medium-grade, and high-grade) were similar. The kinetics of Gadomer-17 in FA also displayed a slower rise-up slope than that in IDC, but the differentiation from low-grade IDC was not as clear as in the Gd-DTPA study. The enhancements in low-grade IDC were much lower than in medium-grade and high-grade IDC. The difference between the medium-grade and high-grade IDC was minimal. In the study of albumin-Gd-DTPA, the relationships among the mean kinetics measured in these four tumor groups were similar to those in the Gadomer-17 study. However, the deviation was larger (30–70% in the albumin-Gd-DTPA study compared with 15–35% in studies using the other two agents), which might degrade the statistical significance.

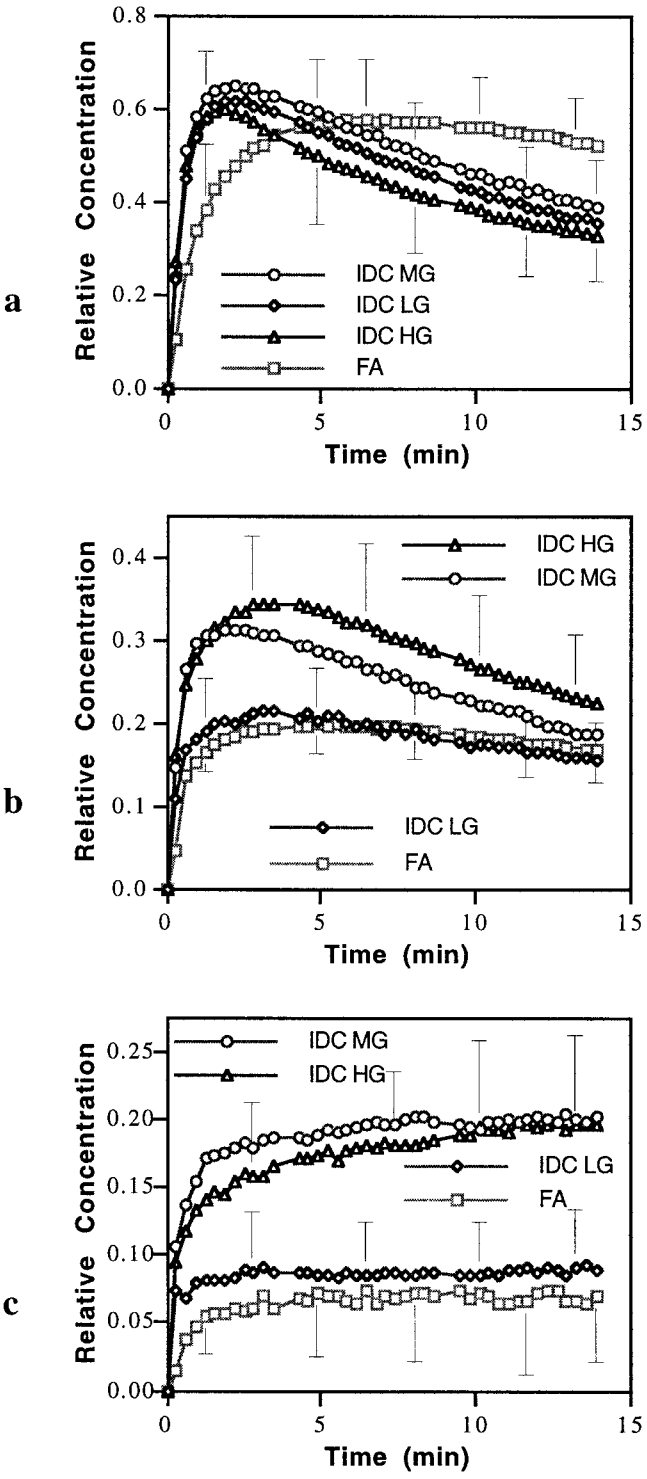

Figure 3. The relative concentration kinetics in the four tumor groups: FA, LG, MG, and HG-IDC, by using Gd-DTPA **(a)**, Gadomer-17 **(b)**, and albumin-Gd-DTPA **(c)**, respectively. The vertical axis is the relative concentration defined as the measured enhancement normalized to the enhancement in the liver at 0.6 min after injection (in Fig. 2). The kinetics of Gd-DTPA showed a slower rise-up slope and a slower decay rate in FA than in IDC and were similar in the three IDC groups. The kinetics of Gadomer-17 could differentiate the LG-IDC from the MG and HG-IDC. In the albumin-Gd-DTPA study, FA also showed a slower rise-up slope than IDC, and the LG-IDC was clearly separated from the MG and HG-IDC. The variations in the three IDC groups were comparable, 15–30% (the range over the time points) in the Gd-DTPA study, 20–35% in the Gadomer-17 study, and 30–45% in the albumin-Gd-DTPA study. In the FA group, the variations were 20–35% in the Gd-DTPA study, 15–20% in the Gadomer-17 study, and as high as 70% in the albumin-Gd-DTPA study. The error bars show the standard deviations in the FA, LG, and HG-IDC groups at some time points.

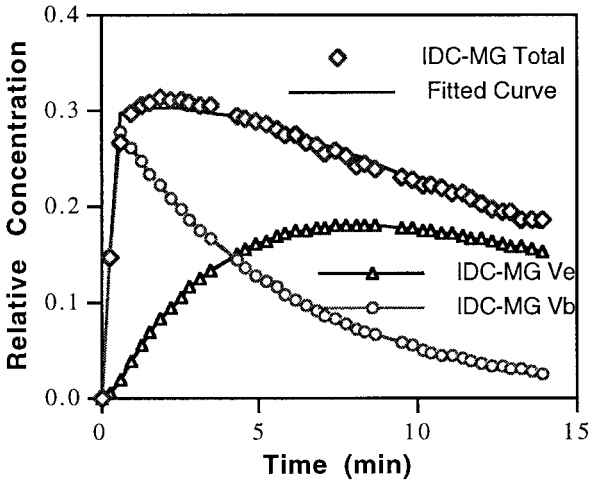

Figure 4. An example of the pharmacokinetic analysis of separation of the vascular (Vb) and extravascular (Ve) components in the kinetics of Gadomer-17 (Total) measured in the medium-grade IDC group. The vascular component was mainly determined by the up-slope. Since the vascular component decays fast, at later time the distribution was mostly in the extravascular space. The kinetic curve could be fitted well with the two-compartmental pharmacokinetic model, as demonstrated by the solid curve.

In each tumor the kinetics measured by each agent were analyzed with a two-compartmental pharmacokinetic model to derive three fitting parameters (V_b, V_eK_{12}, and K_{21}), and to separate the vascular and extravascular components. The analysis procedure has been described in our previous publications (19,20). Figure 4 shows an example of the analysis in the kinetics of Gadomer-17 measured in the medium-grade IDC group. The vascular component in the kinetics was determined by the rising segment of the curve. The decay in the vascular kinetics was determined by the decay rate in the blood concentration. The extravascular component was related to the vascular component with in-flux and out-flux transport rates (K_{12} and K_{21}) from vessel to the interstitial space and the distribution volume in the interstitial space (V_e). As shown, the kinetic curve could be fitted extremely well with the two-compartmental pharmacokinetic model.

The mean vascular volumes (V_b) in the four tumor groups as derived from the kinetics of the three agents are listed in Table 1. The number shown is the fractional vascular volume, in terms of percentage. In all four groups, the volume derived from the kinetics of Gd-DTPA was higher than that of Gadomer-17, and the volume derived from the kinetics of albumin-Gd-DTPA was the lowest. As shown in Fig. 3, the vascular volume was determined by the rising slope; it not only included the true vascular volume but also the early leakage volume in the interstitial space. Therefore, the derived vascular volume could be more appropriately termed as *apparent vascular volume*, and the volume measured by the largest agent (albumin-Gd-DTPA) was more reliable than that measured by the other two smaller agents. Vascular volume analyzed from the kinetics of albumin-Gd-DTPA showed that the high-grade IDC had a 1.5-fold higher vascular volume than the low-grade IDC, and the low-grade IDC had a 2.3-fold higher vascular volume than FA (both significant), unlike the results measured by the other two (smaller) agents. The vascular volume measured by Gd-DTPA showed a significant difference between FA and LG-IDC, but not between LG and HG IDC. In contrast, the vascular volume measured by Gadomer-17 showed a significant difference between LG and HG IDC, but not between FA and LG IDC. Figure 3 shows that enhancement kinetics of the three agents in FA all demonstrated a slower initial enhancement, which was due to its smaller vascular volume. The mean out-flux transport rate (K_{21}) in the four tumor groups are listed in Table 2. While the deviations are small in Gd-DTPA studies, they are large in the studies of the two macromolecular agents. In the Gd-DTPA study, the overall mean K_{21} in IDC was 0.30 ± 0.09 (1/min), which was significantly greater than that in FA, 0.13 ± 0.04 (1/min).

In addition to each individual tumor, the curves (mean kinetics of each group) shown in Fig. 3 were also analyzed, and the derived extravascular kinetics from fitting are shown in Fig. 5.

Since the vascular component also includes the early leakage volume, the extravascular component shown in Fig. 5 is actually the kinetics in the slow leakage volume in the interstitial space. However, this still provides information about the transport of agents into the extravascular space. In the extravascular kinetics of Gd-DTPA, the initial distribution was faster in IDC than FA. Five minutes after the injection, while the contrast agent in IDC had started to decay, the extravascular distribution in FA still remained high, even higher than that in IDC. In terms of pharmacokinetic parameters, the slower decay was reflected by the smaller out-flux transport rate K_{21}. The extravascular kinetics of Gadomer-17 and albumin-Gd-DTPA demonstrated a similar trend, which was different from the Gd-DTPA results. In both studies, the extravascular concentration was the highest in HG IDC, and then, in descending

Table 1
Fractional Vascular Volume (V_b) Derived From the Kinetics of the Three Agents in the Four Tumor Groups (%)

Agent	FA	IDC		
		LG	MG	HG
Gd-DTPA	3.7 ± 1.9*	8.4 ± 1.8	9.6 ± 3.3	10 ± 3.2
Gadomer-17	3.1 ± 1.5	4.1 ± 1.5**	6.6 ± 1.3	5.9 ± 1.5
Albumin-Gd-DTPA	0.9 ± 0.6*	2.0 ± 0.9**	3.7 ± 1.4	3.1 ± 1.1

*V_b in FA is significantly lower than that in LG IDC.
**V_b in LG IDC is significantly lower than that in HG IDC.

Table 2
Out-flux Transport Rate (K_{21}) Derived From the Kinetics of the Three Agents in the Four Tumor Groups (1/min)

Agent	FA	IDC		
		LG	MG	HG
Gd-DTPA	0.13 ± 0.04*	0.32 ± 0.08	0.28 ± 0.11	0.28 ± 0.09
Gadomer-17	0.11 ± 0.13	0.07 ± 0.03	0.09 ± 0.03	0.09 ± 0.06
Albumin-Gd-DTPA	0.33 ± 0.40	0.03 ± 0.05	0.33 ± 0.40	0.14 ± 0.14

K_{21} in FA is significantly smaller than that in the three IDC groups.

order, MG IDC, FA, and LG IDC. The difference between HG and MG IDC could be better appreciated by Gadomer-17, and the difference between LG IDC and FA could be better appreciated by albumin-Gd-DTPA. The results of the albumin-Gd-DTPA study (Fig. 5c) demonstrate that in FA the agents can quickly leak out from the vessels into the interstitial space, while in LG IDC the agents can only slowly leak out from the vessels. Transport was the easiest in HG IDC; a large amount of this agent can easily diffuse into the interstitial space.

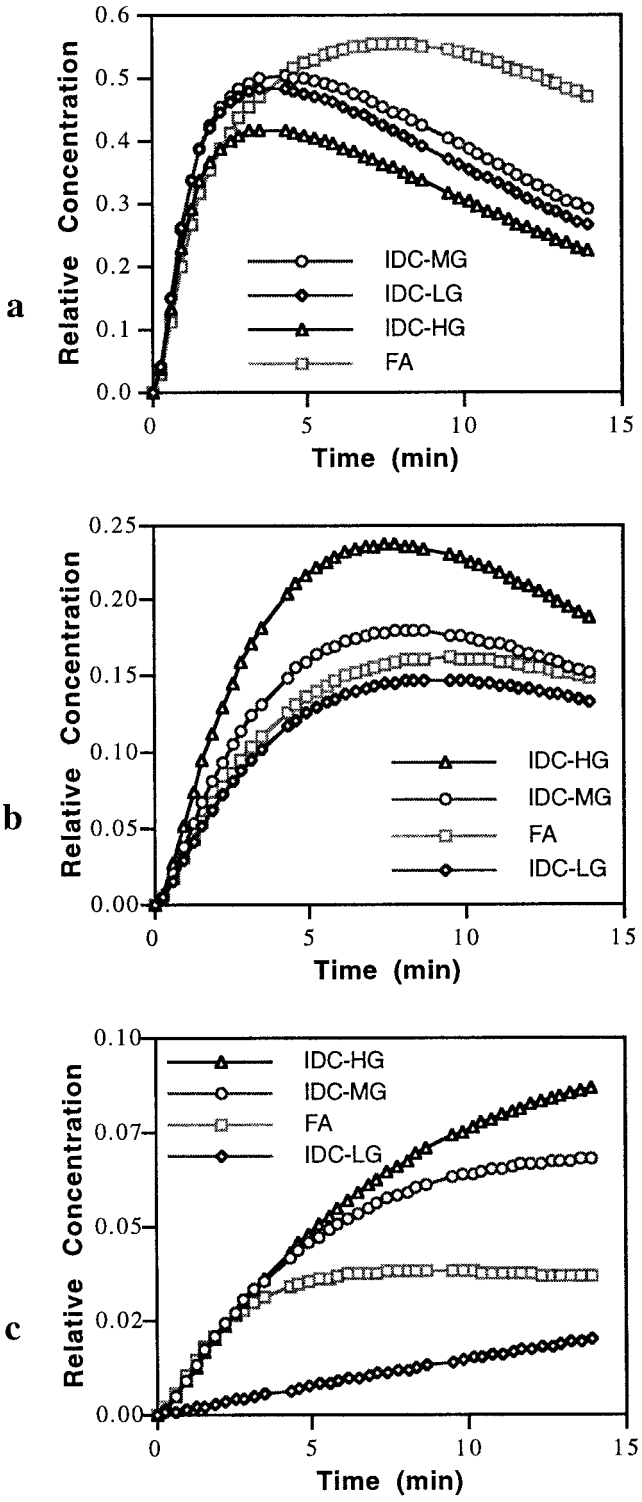

Table 3
Differentiation Between FA and Low-Grade (LG) IDC and Between Low-Grade IDC and High-Grade (HG) IDC From the Kinetics of the Three Contrast Agents

Agent	FA vs. LG IDC	LG vs. HG IDC
Gd-DTPA		
Whole tumor kinetics	<2 or >8 min*	NS
Vascular volume	—*	NS
Extravascular kinetics	>7 min*	NS
Gadomer-17		
Whole tumor kinetics	NS	>1 min*
Vascular volume	NS	—*
Extravascular kinetics	NS	<13 min*
Albumin-Gd-DTPA		
Whole tumor kinetics	NS	>2 min*
Vascular volume	—*	—*
Extravascular kinetics	<10 min*	>0 min*

*Significant difference ($P < 0.05$) in the given time window after the injection. NS, not significant.

Separation between LG and HG IDC was very clear in the extravascular kinetics. Although FA had a lower vascularity, it had a high interstitial space volume, which facilitated the gradual delivery of all three agents into the tumor.

Results of the statistical analysis based on the measured kinetics from the whole tumor, the vascular volume, and the extravascular kinetics are summarized in Table 3. The whole tumor kinetics shown in Fig. 3 and the extravascular kinetics shown in Fig.5 were used in the analysis. The significant time window after injection of contrast agent is also indicated. The vascular volume results are from Table 1. We focused our attention on the differentiation between FA and LG IDC, and on the differentiation between LG IDC and HG IDC. The kinetics measured from MG and HG IDC were similar (as shown in Figs. 3 and 5); they were thus considered indifferentiable and were not further analyzed with statistical tests. We note that Gd-DTPA (whole tumor or vascular or extravascular components) could differentiate FA from IDC, but could not differentiate between LG and HG IDC. In the Gadomer-17 study, the whole tumor kinetics and the derived vascular volume and extravascular kinetics all revealed significant differences between LG and HG IDC. The kinetics between FA and LG IDC were not significantly different. In the albumin-Gd-DTPA study, the measured kinetics and the derived

Figure 5. The extravascular kinetics (or the kinetics in the slow leakage volume in the interstitial space) derived from pharmacokinetic analysis of the relative concentration curves shown in Fig. 3 (the mean kinetics in each group). The symbols were displayed for ease of comparison with Fig. 3 and did not present real data points. In the extravascular kinetics of Gd-DTPA **(a)**, the initial distribution was faster in IDC than in FA, but 5 min after injection the concentration in FA became higher than in IDC. The extravascular kinetics of Gadomer-17 **(b)** and albumin-Gd-DTPA **(c)** demonstrated a similar trend, the highest in the HG-IDC, and then, in descending order, MG-IDC, FA, and LG-IDC. The difference between HG and MG-IDC could be better noted by Gadomer-17, and the difference between LG-IDC and FA could be better appreciated by albumin-Gd-DTPA.

vascular and extravascular kinetics all revealed significant differences between LG and HG IDC. The kinetics measured between FA and LG IDC were not significantly different due to large variations in FA. However, after performing pharmacokinetic analysis to separate the vascular and extravascular components, both revealed significant differences.

DISCUSSION

Tumor Model

We established a carcinogen-induced animal tumor model to grow malignant and benign tumors, and we studied the pharmacokinetic characteristics of three contrast agents. In the rat, ENU induces primarily IDC breast cancer (as in humans), and also primarily FA benign breast tumors (also as in humans) (21). ENU-induced rat breast IDCs also show a range of morphological changes, from well-differentiated proliferations of tubules with minimal stromal invasion (eg, Fig. 1a) to highly infiltrative, poorly differentiated, and rapidly dividing tumors (eg, Fig. 1c). In humans, these morphological variations can be assigned a numerical score that strongly correlates with tumor aggressiveness and patient survival (25). Since the goal of this study was to predict not only benign versus malignant behavior by MRI, but also degrees of aggressiveness among the malignant tumors, the grade of each tumor was compared with the MRI characteristics of each contrast agent.

Differential Diagnosis Based on Whole Tumor Kinetics

In humans, the kinetics of Gd-DTPA in FAs have been reported to show a slower up-slope and a slower decay rate than that in malignant tumors (1,2). In the current study, we also observed a similar pattern. In FA the kinetics of Gd-DTPA displayed a slower up-slope and a slower decay rate. The early enhancement (less than 2 minutes) in FA was lower than in IDC, and later (after 8 minutes) it became higher than in IDC. This finding could be interpreted to mean that FA has a lower vascular volume and a higher interstitial space volume than IDC (see later discussion). Therefore, if the post Gd-DTPA enhanced images are used to differentiate FA from IDC, the timing is critical. On the other hand, the kinetics of Gd-DTPA failed to differentiate among IDCs of various grades. In contrast to Gd-DTPA, the kinetics of the medium-size agent Gadomer-17 could differentiate between LG and HG IDC, but could not separate FA from LG IDC. The kinetics of albumin-Gd-DTPA also displayed a significant difference between LG and HG IDC, and the separation between FA and LG IDC was not significant due to the relatively high variations in FA. The high degree of variation could be partly attributed to the low signal-to-noise ratio (SNR) but also might be due to various types of FAs that were pooled together. FAs in humans have also been known to occur as various types (31). The results suggest that macromolecular agents may be superior to Gd-DTPA in differential diagnosis of tumor grades, but not in differential diagnosis of FA from IDC. The reason why macromolecular agents can differentiate IDC of low and high grade is presumably the different degree of vascular permeability (or the leakage status of the vessels), which can be better illustrated after separating the vascular and extravascular components in the measured enhancement kinetics, as discussed later.

Interpretation of the Parameters Derived From Pharmacokinetic Analysis

In the present study, a two-compartmental pharmacokinetic model was applied to separate the vascular and extravascular kinetics. Three major factors determine the kinetics of contrast agents in a tissue: blood perfusion, transport of agents across the vessel wall (via diffusion or convection), and diffusion of agents in the interstitium. If the agents delivered by blood are not sufficient, blood perfusion will be the dominant factor in determining the kinetics of agent in the tissue. If the agents delivered by the blood supply are sufficient, then the second factor, transport across the vessel wall (mainly through diffusion for the agents used in this study), comes into play. Transendothelial transport is described by the permeability-surface area product (PS), which is dependent on the width of junctions between endothelial cells or pathways through the transendothelial vesicles, as well as the total surface area available for exchange (15). The third factor is the diffusion of agents away from the vascular space and within the interstitium (32). Although the three factors cannot be clearly separated in the measured pharmacokinetics, they must be considered when one is attempting to interpret the derived pharmacokinetic parameters as the real physiological parameters.

Differential Diagnosis Based on the Derived Vascular Volume

In the pharmacokinetic analysis, the initial rising phase in the measured enhancement time course after contrast agent injection is attributed to vascular contribution. In the present study the vascular contribution was converted to the fractional vascular volume by using the liver as a reference. In the albumin-Gd-DTPA study, the vascular volume showed a significant difference between FA and LG IDC (2.3-fold) and also between LG and HG IDC (1.5-fold). These two findings were not fully revealed by the smaller agents, Gd-DTPA or Gadomer-17, presumably due to their inability to measure the real vascular volume. In the Gd-DTPA study, the vascular volume was significantly different between FA and LG IDC, but not between LG IDC and HG IDC, whereas in the study of Gadomer-17, the vascular volume was significantly different between LG and HG IDC, but not between FA and LG IDC. Our previous experience in analyzing the kinetics of Gd-DTPA and other macromolecular contrast agents has shown that the derived vascular compartment is actually an apparent vascular volume (23,33), which includes the true vascular volume and the fast leakage volume in the interstitial space; these are inseparable due to quick equilibrium of agents between them. The fast leakage volume was

determined by how easily the agent can leak into the interstitial space, which in turn was dependent on the relative size of the agent and the endothelial gap on the vessel wall. Therefore, the problem was more severe when using a smaller agent than a macromolecular agent. The data presented in Table 1 also demonstrate that the vascular volume derived from the kinetics of smaller agents was higher. Therefore, the vascular volume derived from albumin-Gd-DTPA was more reliable than that derived from the other two smaller agents, since it contained less early leakage volume.

Differential Diagnosis Based on the Out-Flux Transport Rate K_{21}

The other parameter analyzed in the model is the out-flux transport rate K_{21} from the interstitial space back into the vascular space. The out-flux transport rate K_{21} (or the exchange rate between vascular and extravascular space) has been reported to be the best parameter for differentiating FAs from malignant tumors (8,9). However, interpretation of this parameter as vascular permeability must be done cautiously. In addition to dependence on the PS (product of vascular permeability and surface area), the K_{21} is also a measure of how fast the agent diffuses from the interstitial space back to vessels, which is determined by the relative interstitial distribution volume versus the vascular volume. Based on this parameter, the only significant difference is between FA and IDC in the Gd-DTPA study (0.13 ± 0.04/min for FA vs. 0.30 ± 0.09/min for IDC). The smaller K_{21} suggested that in FA it had a relatively small vascular volume but a large interstitial distribution volume compared with that in IDC. In the Gadomer-17 and albumin-Gd-DTPA studies, the variation of the K_{21} values within each tumor group was very large (in the range of 50–150%), which greatly degraded the statistical significance when this parameter was tested for differential diagnosis.

Differential Diagnosis Based on Extravascular Kinetics

The extravascular kinetics derived from pharmacokinetic analysis showed the distribution of agents into the interstitial space (excluding the early leakage portion). Gd-DTPA is a small (or so-called free-diffusable) agent; thus it was expected to be distributed into the entire interstitial space except in necrotic regions. In our analysis the necrotic region was excluded in the tumor ROI based on T_2-weighted images and thus could not bias the results. From the extravascular distribution of Gd-DTPA shown in Fig. 5, we note that the LG and MG IDC had a similar interstitial space volume, which was smaller (not significantly) in HG IDC and larger (significantly) in FA. The findings correlate with the expected cell volume: more cells in HG IDC and less cells in FA. Statistical analysis indicates that the extravascular kinetics of Gd-DTPA could be used to differentiate FA from IDC, but it failed to show any significant differences among IDCs of various grades, presumably because of non-selectivity of vessels to Gd-DTPA.

As discussed above, the amount of contrast agent transported across the vessel wall is governed by perfusion and vascular permeability. The amount of contrast agent that accumulated in the interstitial space is also dependent on the interstitial space volume. Since the vascular volume in the three IDC groups only differed by less than 1.5-fold, and their interstitial space volumes were comparable according to results of Gd-DTPA, the differences in the extravascular kinetics in the three IDC groups measured by Gadomer-17 and albumin-Gd-DTPA were attributed to vascular permeability. Figure 5b and c demonstrates that transport of Gadomer-17 and albumin-Gd-DTPA into the interstitial space was the easiest and greatest in HG IDC, was lesser in MG IDC and FA, and was the most difficult in LG IDC. As the degree of malignancy increases, the vessels might become leakier due to more secretion of angiogenic factors, eg, vascular endothelial growth factor (17,34). The similar findings observed in Gadomer-17 and albumin-Gd-DTPA studies suggested that agents of their sizes could selectively diffuse across the vessel wall, more in the HG than in the LG IDC. However, the difference between MG and HG IDC was not significant. If the analyses were performed by correlating the kinetics of each individual tumor with its own grade, a linear relationship across the LG, MG, and HG groups, as reported by Daldrup et al (35) might not be found. The inconsistency may be due to tumor inhomogeneity. The MG and HG tumors grew much faster than the LG tumors. Tumor size at the time of experiment varied from 1.5 to 3.5 cm in diameter. In the MRI experiment we were able to cover the entire tumor; however, the pathological examination could only randomly sample certain regions. For example, if a tumor had two Scarf-Bloom-Richardson grades of 4 and 7, the averaged score (5.5) would assign the tumor to the MG group. However, the unsampled high-grade region might be dominant in the tumor, and this tumor should belong to the HG group. In contrast, the scores in LG and HG tumors displayed little variation across various regions. The sampling problem in the MG group might be the factor causing overlapping with the HG group.

The findings in the current study also seemed to contradict those reported by Adam et al (18) regarding the differential diagnosis between benign and malignant tumors using Gd-DTPA. They reported that Gadomer-17, but not Gd-DTPA, could differentiate benign from malignant tumors. In their study the benign tumors consisted of epithelial and connective tissue components (in nine dogs) and benign adenomas (in four dogs), whereas in ours only fibroadenoma was included. In some other benign tumors in our study (eg, fibroma), we observed strong Gd-DTPA enhancement but weak Gadomer-17 enhancement. If they were included in the benign group, the mean Gd-DTPA enhancement would be higher and the Gadomer-17 enhancement would be lower, and the finding might be reversed. Another potential factor was the necrosis in the malignant tumors. In the IDC, especially HG, some necrotic regions existed that were excluded from our analysis. If they were not excluded, the Gd-DTPA enhancement in

IDC would be lower, and the separation from FA might become smaller, even non-significant.

The results of Gd-DTPA indicated that FA had a higher interstitial space volume than IDC. The two macromolecular agents (Gadomer-17 and albumin-Gd-DTPA) entered MG and HG IDC more easily than FA even though the smaller interstitial space volume suggested that the vessels in the MG and HG IDC are leakier than in FA. The extravascular kinetics of albumin-Gd-DTPA in FA and LG IDC showed that the agent could only slowly diffuse into the LG IDC but that diffusion was much easier in FA. The extravascular kinetics of Gadomer-17 showed no significant difference between them. The reason why macromolecular agents could enter FA more easily than LG IDC might be its higher interstitial space volume (which may also be associated with lower interstitial pressure). The degree of vascular permeability differences between FA and LG IDC could not be assessed from our data.

CONCLUSIONS

The results measured by using the three contrast agents, with or without pharmacokinetic analyses, are summarized in Table 3, which shows that that the clinically available small agent (Gd-DTPA) could be used to differentiate FA from the malignant tumors. Without performing dynamic imaging and pharmacokinetic analysis, the significant difference could be detected within the first 2 and 8 minutes after injection. With pharmacokinetic analysis, the derived vascular volume and the out-flux transport rate K_{21} showed a significant differentiation. Therefore, when Gd-DTPA is used to differentiate FA from IDC based on post-enhanced images, timing is an important factor. Gd-DTPA could not differentiate between malignant tumors of low and high grades, presumably due to their similar vascular volume (1.5-fold difference), their similar interstitial space volume, and the non-selectivity of vessels for passage of Gd-DTPA.

The two macromolecular agents revealed significant differences in the extravascular kinetics of LG and HG IDC. Since their interstitial space volumes are comparable, the results can be interpreted to mean that HG IDC has a much higher vascular permeability than LG IDC. Since Gadomer-17 can be cleared quickly via kidneys and the tolerance dose is high, it may be a suitable agent for tumor staging in humans. However, Gadomer-17 could not differentiate between LG IDC and benign FA, due to the similar enhancement patterns in tumors with relatively low vascular but high extravascular components (FA), and in those with a relatively high vascular but low extravascular components (LG IDC). The vascular permeability differences between FA and LG IDC could not be determined.

The largest agent, albumin-Gd-DTPA, was capable of differentiating LG IDC from HG IDC (from measured kinetics or pharmacokinetic analysis) and also of differentiating FA from LG IDC (only from pharmacokinetic analysis). The vascular volume derived from this largest agent was more reliable than the other two agents. It indicated that HG IDC had a higher vascular volume than that of LG IDC (significant) and that FA had the lowest vascular volume (significantly lower than that of LG IDC). Its extravascular kinetics also displayed significant differences between LG and HG IDC; therefore, it could also be used for tumor staging. However, the low SNR (resulting in high variability) was its major technical concern. Other biological concerns, eg, protein poisoning, further limited the suitability of this agent for human use. The results in this ENU-induced animal tumor model suggest that the macromolecular agents provide useful information for differential diagnosis among IDC of various grades, but they do not provide information superior to that of Gd-DTPA for differential diagnosis between IDC and FA.

ACKNOWLEDGMENTS

The authors thank Schering AG and Dr. H.-J. Weinmann for providing us with the macromolecular contrast agent Gadomer-17. We thank Dr. Mohammed Bozorgzadeh for the synthesis of N-ethyl-N-nitrosourea.

REFERENCES

1. Kaiser WA, Zeitler E. MR imaging of the breast: fast imaging sequences with and without Gd-DTPA. Preliminary observations. Radiology 1989;170:681–686.
2. Gribbestad IS, Nilsen G, Fjosne H, et al. Contrast-enhanced magnetic resonance imaging of the breast. Acta Oncol 1992;31:833–842.
3. Flickinger FW, Allison JD, Sherry RM, Wright JC. Differentiation of benign from malignant breast masses by time-intensity evaluation of contrast enhanced MRI. Magn Reson Imaging 1993;11:617–620.
4. Orel SG, Schnall MD, LiVolsi VA, Troupin RH. Suspicious breast lesions: MR imaging with radiologic-pathologic correlation. Radiology 1994;190:485–493.
5. Heywang-Kobrunner SH. Contrast-enhanced magnetic resonance imaging of the breast. Invest Radiol 1994;29:94–104.
6. Kelcz F, Santyr G. Gadolinium-enhanced breast MRI. Crit Rev Diagn Imaging 1995;36:287–338.
7. Heywang-Kobrunner SH, Viehweg P, Heinig A, Kuchler C. Contrast-enhanced MRI of the breast: accuracy, value, controversies, solutions. Eur J Radiol 1997;24:94–108.
8. Mussurakis S, Buckley DL, Drew PJ, et al. Dynamic MR imaging of the breast combined with analysis of contrast agent kinetics in the differentiation of primary breast tumours. Clin Radiol 1997;52:516–526.
9. den Boer JA, Hoenderop RK, Smink J, et al. Pharmacokinetic analysis of Gd-DTPA enhancement in dynamic three-dimensional MRI of breast lesions. J Magn Reson Imaging 1997;7:702–715.
10. Heywang-Kobrunner SH, Schlegel A, Beck R, et al. Contrast-enhanced MRI of the breast after limited surgery and radiation therapy. J Comput Assist Tomogr 1993;17:891–900.
11. Whitehouse GH, Moore NR. MR imaging of the breast after surgery for breast cancer. Magn Reson Imaging Clin North Am 1994;2:591–603.
12. Mussurakis S, Buckley DL, Bowsley SJ, et al. Dynamic contrast-enhanced magnetic resonance imaging of the breast combined with pharmacokinetic analysis of gadolinium-DTPA uptake in the diagnosis of local recurrence of early stage breast carcinoma. Invest Radiol 1995;30:650–662.
13. Murray AD, Redpath TW, Needham G, Gilbert FJ, Brookes JA, Eremin O. Dynamic magnetic resonance mammography of both breasts following local excision and radiotherapy for breast carcinoma. Br J Radiol 1996;69:594–600.
14. Rieber A, Merkle E, Zeitler H, et al. Value of MR mammography in the detection and exclusion of recurrent breast carcinoma. J Comput Assist Tomogr 1997;21:780–784.
15. Jain RK. Transport of molecules across tumor vasculature. Cancer Metast Rev 1987;6:559–593.

16. Dvorak HF. Leaky tumor vessels: consequences for tumor stroma generation and for solid tumor therapy. In: Effects of therapy on biology and kinetics of the residual tumor, Part A: pre-clinical aspects. New York: Wiley-Liss Inc.; 1990. p 317–330.
17. Dvorak HF, Brown LF, Detmar M, Dvorak AM. Vascular permeability factor/vascular endothelial growth factor, microvascular hyperpermeability, and angiogenesis. Am J Pathol 1995;146:1029–1039.
18. Adam G, Muhler A, Spuntrup E, et al. Differentiation of spontaneous canine breast tumors using dynamic magnetic resonance imaging with 24-gadolinium-DTPA-cascade-polymer, a new blood-pool agent. Preliminary experience. Invest Radiol 1996;31:267–274.
19. Su MY, Mühler A, Lao X, Nalcioglu O. Tumor characterization with dynamic contrast enhanced MRI using MR contrast agents of various molecular weights. Magn Reson Med 1998;39:259–269.
20. Su MY, Jao JC, Nalcioglu O. Measurement of vascular volume fraction and blood-tissue permeability constants with a pharmacokinetic model: studies in rat muscle Magn Reson Med 1994;32:714–724.
21. Stoica G, Koestner A, Capen CC. Neoplasms induced with high single doses of N-ethyl-N-nitrosourea in 30-day-old Sprague-Dawley rats, with special emphasis on mammary neoplasia. Anticancer Res 1984;4:5–12.
22. Werner EA. The constitution of carbamides. Part IX, The interaction of nitroso acid and mono-substituted ureas. J Chem Soc 1919;115: 1093.
23. Su MY, Najafi AA, Nalcioglu O. Regional comparison of tumor vascularity and permeability parameters measured by albumin-Gd-DTPA and Gd-DTPA. Magn Reson Med 1995;34:402–411.
24. Russo J, Russo IH, Rogers AE, van Zwieten MJ, and Gusterson B. Tumour of the mammary gland in US. In: Turusov VS, Mohr U, editors. Pathology of tumours in laboratory animals. Vol 1. Tumours of the rat. Lyon, France: International Agency for Research on Cancer; 1990. p 47–78.
25. Simpson JF, Page DL. Status of breast cancer prognostication based on histopathologic data. Am J Clin Pathol 1994;102(suppl 1):S3–S8.
26. Tofts PS. Modeling tracer kinetics in dynamic Gd-DTPA MR imaging. J Magn Reson Imaging 1997;7:91–101.
27. Larsson HB, Stubgaard M, Frederiksen JL, Jensen M, Henriksen O, Paulson OB. Quantitation of blood-brain barrier defect by magnetic resonance imaging and gadolinium-DTPA in patients with multiple sclerosis and brain tumors. Magn Reson Med 1990;16:117–131.
28. Tofts PS, Kermode AG. Measurement of the blood-brain barrier permeability and leakage space using dynamic MR imaging. 1. Fundamental concepts. Magn Reson Med 1991;17:357–367.
29. Brix G, Semmler W, Port R, Schad LR, Layer G, Lorenz WJ. Pharmacokinetic parameters in CNS Gd-DTPA enhanced MR imaging. J Comput Assist Tomogr 1991;15:621–628.
30. Shames DM, Kuwatsuru R, Vexler V, Muhler A, Brasch RC. Measurement of capillary permeability to macromolecules by dynamic magnetic resonance imaging: a quantitative noninvasive technique. Magn Reson Med 1993;29:616–622.
31. Hochman MG, Orel SG, Powell CM, Schnall MD, Reynolds CA, White LN. Fibroadenomas: MR imaging appearances with radiologic-histopathologic correlation. Radiology 1997;204:123–129.
32. Baxter LT, Jain RK. Transport of molecules in the tumor interstitium: a review. Cancer Res 1987;47:3030–3051.
33. Su MY, Lao X, Nalcioglu O. Quantitative comparison of pharmacokinetics of polylysine-Gd-DTPA, Gd-DTPA-24-cascade-polymer, and Gd-DTPA in blood, liver, and tumor of rats. In: Proceedings of the 4th SMR Annual Meeting, New York, 1996. p 1697.
34. Claffey KP, Robinson GS. Regulation of VEGF/VPF expression in tumor cells: consequences for tumor growth and metastasis. Cancer Metast Rev 1996;15:165–176.
35. Daldrup H, Shames DM, Wendland M, et al. Correlation of dynamic contrast-enhanced magnetic resonance imaging with histologic tumor grade: comparison of macromolecular and small-molecular contrast media. Pediatr Radiol 1998;28:67–78.